Fifth International Conference on
Recent Advances in Geotechnical Earthquake Engineering and Soil Dynamics
and Symposium in Honor of Professor I.M. Idriss
May 24-29, 2010 • San Diego, California

PROCEDURE TO EVALUATE LIQUEFACTION-INDUCED LATERAL SPREADING BASED ON SHEAR WAVE VELOCITY

Fred (Feng) Yi
Senior Geotechnical Engineer, C.H.J. Incorporated, Colton, CA-USA 92324

ABSTRACT

Evaluation of liquefaction-induced lateral spreading is very important for the design of structures located on gently sloping ground and with relatively shallow groundwater. Extensive research has been performed on the calculation of liquefaction-induced lateral spreading based on the standard penetration test (SPT) and cone penetration test (CPT) data by various researchers (Bartlett and Youd 1992, 1995, Rauch, 1997; Zhang et al., 2004; Idriss and Boulanger, 2008). However, few published papers can be found that address the calculation of liquefaction-induced lateral spreading based on shear wave velocity. This paper presents a procedure to evaluate liquefaction-induced lateral spreading directly based on shear wave velocity. New empirical relationships for factor of safety against liquefaction, maximum shear strain, and shear wave velocity are developed based on the laboratory tests performed at the University of Tokyo (Ishihara and Yoshimine 1992, Yoshimine et al. 2006). The results calculated utilizing this new procedure are compared with those based on SPT and CPT data using existing methods. The results indicate good agreement. This approach not only provides a new method for estimating the liquefaction-induced lateral spreading directly from shear wave velocity data but also provides a cost effective tool for verification of CPT results because of the small cost increase in measuring shear wave velocity during the standard CPT testing.

INTRODUCTION

As one of the major surficial manifestations of liquefaction, lateral spreading has been observed in nearly all major earthquakes from the 1923 Kanto earthquake in Japan (Hamada et al. 1992) to the recent Sichuan earthquake in China (Wang 2008). "Damage caused by lateral spreads, though seldom catastrophic, is severely disruptive and often pervasive. … Cumulatively, more damage has been caused by lateral spreads than by any other form of liquefaction-induced ground failure." (NRC, 1985). Due to the enormous damage to engineered structures and lifelines caused by liquefaction-induced lateral spreading, its evaluation and prediction becomes very important for the design and construction of structures located on areas susceptible to lateral spreading. These areas are usually relatively flat, along waterfronts, and attractive for urban development (Rauch, 1997). Since the late 1980's, extensive research has been performed on the calculation of liquefaction-induced lateral spreading (NRC, 1985, Hamada et al. 1986, Bartlett and Youd 1992, 1995, Rauch, 1997, Zhang et al., 2004; Idriss and Boulanger, 2008). Several methods have been proposed by individuals to predict the liquefaction-induced lateral spreading. These methods include empirical methods based on a database from observed case histories (Bartlett and Youd 1995, Rauch, 1997), semi-empirical methods based on laboratory test results, field exploratory data and anticipated earthquake magnitude (Zhang et al., 2004; Idriss and Boulanger, 2008), and numerical simulation using the finite element method (FEM) and finite-difference method (FDM) (Valsamis et al. 2007).

Several in-situ testing methods are in common usage for exploration of subsurface soils, including the standard penetration test (SPT), the cone penetration test (CPT), shear-wave velocity measurements (V_s), and the Becker penetration test (BPT). All of these methods have been utilized in the evaluation of liquefaction potential. Most of the currently published methods for evaluating liquefaction-induced lateral spreading are based on either SPT or CPT data. Few published papers can be found that address the calculation of liquefaction-induced lateral spreading based on shear wave velocity. This paper presents an approach for estimating liquefaction-induced lateral spreading based on shear wave velocity. This approach includes a detailed procedure for calculating the factor of safety against liquefaction and the maximum cyclic shear strain. The proposed method was

evaluated by comparing the results calculated based on SPT and CPT data utilizing currently widely accepted methods.

GEOLOGIC CONDITIONS FOR LATERAL SPREADING

Liquefaction-induced lateral spreading is defined as the finite, lateral displacement of gently sloping ground as a result of pore pressure build-up or liquefaction in a shallow underlying deposit during an earthquake (Rauch, 1997). A three dimensional description of the lateral spreading is illustrated in Fig. 1 (Varnes 1978, Rauch 1997). Fig. 2 shows two typical patterns of soil liquefaction and the induced lateral spreading.

The geologic conditions for increased susceptibility to liquefaction-induced lateral spreading are: 1) shallow water table, 2) presence of unconsolidated loose sandy alluvium, typically Holocene in age; 3) strong ground shaking, and 4) constant initial shear stress resulting from a gently sloping ground. The first three conditions are the conditions required for liquefaction to occur. The last is the additional condition for liquefaction-induced lateral spreading to occur. Although not clearly stated in most publications, the estimation of liquefaction-induced lateral spreading is also generally based on these four conditions.

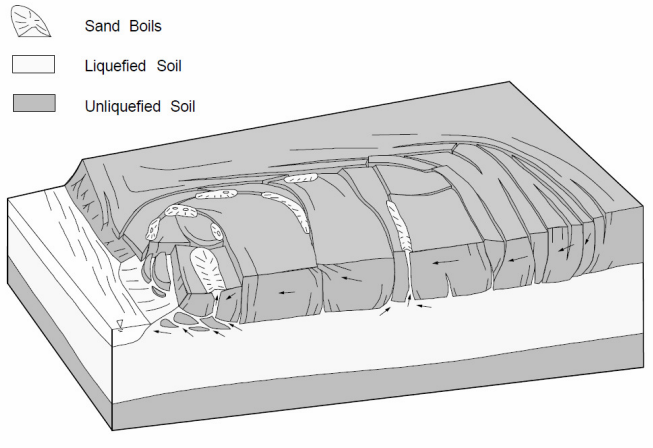

Fig. 1 Schematic depiction of a lateral spreading resulting from liquefaction in an earthquake (after Rauch 1997, originally from Varnes 1978)

PROCEDURES TO EVALUATE LIQUEFACTION-INDUCED LATERAL SPREADING

The procedure presented hereafter is similar to that adopted by Zhang et al. (2004) and includes the following steps:

Step 1. Assess the liquefaction potential based on Andrus and Stokoe's method (Andrus and Stokoe 2000, Andrus et al. 2004).

Step 2. Calculate the maximum shear strain based on results of simple shear tests performed at the University of Tokyo (Ishihara and Yoshimine 1992, Yoshimine et al. 2006) extended for the application to V_s data.

Step 3. Calculate the lateral spreading

The related previous work will be reviewed in the following sections.

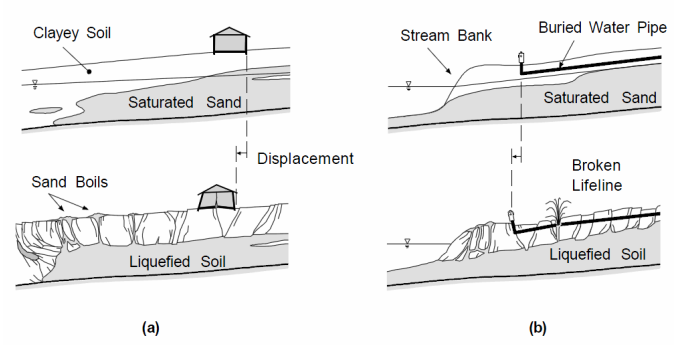

Fig. 2 Soil liquefaction and lateral spreading of (a) gently sloping ground and (b) toward a free face (after Rauch 1997)

Evaluation of factor of safety against liquefaction

The factor of safety against liquefaction is defined as the ratio of the cyclic resistance ratio, CRR_M, that will cause liquefaction of the soil for a given number of cycles, to the cyclic stress ratio, *CSR*, developed in the soil by the earthquake motion.

$$FS_{liq} = \frac{CRR_M}{CSR} \tag{1}$$

Cyclic stress ratio (CSR). In the simplified procedure (Seed and Idriss 1971), the CSR developed in the soil is calculated by a formula that incorporates ground surface acceleration, total and effective stresses in the soil at different depths (which in turn are related to the location of the ground water table), non rigidity of the soil column, and a number of simplifying assumptions. Seed and Idriss (1971) formulated the following equation for calculation of CSR.

$$CSR = \tau_{av} / \sigma_{v0}' = 0.65(a_{\max} / g)(\sigma_{v0} / \sigma_{v0}')r_d \tag{2}$$

where τ_{av} is the average equivalent uniform cyclic shear stress caused by the earthquake and is assumed to be 0.65 of the maximum induced stress, $a_{\max}$ is the peak horizontal acceleration at ground surface generated by the earthquake, g is the acceleration of gravity, σ_{v0} and σ_{v0}' are total and effective overburden stresses, respectively, and r_d is a stress reduction coefficient.

Several methods have been published by individuals for the calculation of r_d (Seed and Idriss 1971, Lao and Whitman 1986, Seed et al 2003, Idriss 1999). The expression (Eq. 3)

proposed by Idriss (1999) may be used to estimate the average value of r_d.

$$r_d = \exp[\alpha(z) + \beta(z) \cdot M] \quad (3a)$$

$$\alpha(z) = -1.012 - 1.126 \sin\left(z/11.73 + 5.133\right) \quad (3b)$$

$$\beta(z) = 0.106 + 0.118 \sin\left(z/11.28 + 5.142\right) \quad (3c)$$

in which z is the depth below ground surface in meters, M is the earthquake moment magnitude, and the arguments inside the sine terms are in radians.

Cyclic resistance ratio (CRR). Andrus and Stokoe (2000) developed a V_s-based CRR curve for uncemented, Holocene-age soils with 5% or less fines at an earthquake magnitude 7.5 as shown in Eq. 4.

$$CRR_{7.5cs} = 0.022\left[\frac{(V_{s1})_{cs}}{100}\right]^2 + 2.8\left[\frac{1}{215 - (V_{s1})_{cs}} - \frac{1}{215}\right] \quad (4)$$

where subscript *cs* is the abbreviation for clean sand (soils with 5% or less fines), and $(V_{s1})_{cs}$ is the overburden stress-corrected shear wave velocity as defined in Eq. 5 to account for the influences of the state of stress in soil.

$$(V_{s1})_{cs} = K_{cs} V_{s1} = K_{cs} V_s (p_a / \sigma_{v0}')^{0.25} \quad (5)$$

where V_{s1} is the overburden stress-corrected shear wave velocity of sandy soils, p_a is the reference stress of 100 kPa or about atmospheric pressure, and K_{cs} is a fines content (*FC*) correction factor. Juang et al (2002) suggested the following relationships for estimating K_{cs}:

$$K_{cs} = 1.0 \text{ , for } FC \le 5\% \quad (6a)$$

$$K_{cs} = 1 + (FC - 5)T \text{ , for } 5\% < FC < 35\% \quad (6b)$$

$$K_{cs} = 1 + 30T \text{ , for } FC \ge 35\% \quad (6c)$$

where

$$T = 0.009 - 0.0109\left(V_{s1}/100\right) + 0.0038\left(V_{s1}/100\right)^2 \quad (6d)$$

It is preferred that the *FC* measured from SPT samples be used for above corrections. If measured data is not available, *FC* estimated from CPT data could also be used (Yi, 2009).

Research indicates that other corrections, such as earthquake magnitude, overburden pressure, and static shear stress, should also be made to the CRR (Seed and Idriss 1982, Seed 1983, Idriss and Boulanger, 2008). For any earthquake moment magnitude *M*,

$$CRR_M = CRR_{7.5cs}(MSF) K_\sigma K_\alpha \quad (7)$$

where *MSF* is the magnitude scaling factor, and K_σ and K_α are factors for overburden and initial static stress ratio corrections, respectively. Several expressions have been proposed by individuals for these corrections. The most recently published work by Idriss and Boulanger (2008) can be utilized.

Magnitude scaling factor (*MSF*). Various relationships between magnitude scaling factor and earthquake moment magnitude have been proposed (Seed and Idriss 1982, Tokimatsu and Yoshimi, 1983, Arabgo 1996, Idriss 1999). By studying the relations between the number of equivalent uniform stress cycles and earthquake magnitude, Idriss (1999) suggested the magnitude scaling factor as:

$$MSF = 6.9\exp\left(-M/4\right) - 0.058 \le 1.8 \quad (8)$$

Overburden correction factor K_σ. Laboratory cyclic triaxial compression tests show that while liquefaction resistance of a soil increases with increasing confining pressure, the resistance, as measured by the stress ratio, is a nonlinear function that decreases with increased normal stress. Seed (1983) suggested a correction factor, K_σ, to account for this nonlinearity for overburden pressures greater than 100 kPa. Although various expressions for an overburden correction factor have been proposed by a number of researchers, this author recommends the use of K_σ proposed by Boulanger and Idriss (2004).

$$K_\sigma = 1 - C_\sigma \ln\left(\frac{\sigma_{v0}'}{p_a}\right) \le 1.1 \quad (9a)$$

where the coefficient C_σ can be expressed in terms of corrected shear wave velocity.

$$C_\sigma = \frac{1}{18.9 - 3.1\left[(V_{s1})_{cs}/100\right]^{1.976}} \le 0.3 \quad (9b)$$

Static shear stress correction factor K_α. This factor was originally introduced by Seed (1983) to account for the effect of static shear stresses on CRR. In the 1996 NCEER workshop (Youd et al. 1997), it was concluded that the wide ranges in potential K_α values developed in past investigations indicate a lack of consensus and a need for continued research and field verifications, and that general recommendations for use of K_α by the engineering profession are not advisable at this time. Since that workshop, further research has been performed by Idriss and Boulanger (2003a, 2003b). For the purpose of liquefaction-induced lateral spreading evaluation, the author believes that Idriss and Boulanger's results can be used.

$$K_\alpha = \frac{CRR_\alpha}{CRR_{\alpha=0}} = a + b \cdot \exp\left(\frac{-\xi_R}{c}\right) \quad (10a)$$

$$a = 1267 + 636\alpha^2 - 634\exp(\alpha) - 632\exp(-\alpha) \quad (10b)$$

$$b = \exp\left(-1.11 + 12.3\alpha^2 + 1.31\exp(\alpha + .0001)\right) \quad (10c)$$

$$c = 0.138 + 0.126\alpha + 2.52\alpha^3 \quad (10d)$$

$$\alpha = \tau_s / \sigma_{v0}' \quad (10e)$$

$$\xi_R = \frac{1}{Q - \ln\left(100\,p'/p_a\right)} - 0.18\left(\frac{V_{s1cs}}{100}\right)^{1.976} \quad (10f)$$

$$p' = \tfrac{1}{3}(1 + 2K_0)\sigma_{v0}' \quad (10g)$$

where K_0 is the coefficient of lateral earth pressure at rest and Q is a grain type related empirical constant approximately equal to 10 for quartz and feldspar, 8 for limestone, 7 for anthracite, and 5.5 for chalk. In addition, α and ξ_R should be constrained within the following limits.

$$\alpha \le 0.35 \text{ and } -0.6 \le \xi_R \le 0.1 \quad (10h)$$

Liquefaction-induced maximum cyclic shear strains of clean sand

Relative density. To study the volume change characteristics of sand after liquefaction, several series of uni- and multi-directional cyclic simple shear tests have been performed at the University of Tokyo (Ishihara and Yoshimine 1992, Yoshimine et al. 2006). The results indicate that one of the important parameters affecting the cyclic maximum shear strain of liquefied sands is the relative density (D_R) of the sand. To utilize V_s data, a relationship between D_R and V_s is necessary. Existing relationships between D_R and V_s are not available in published research. However, this relationship can be established by utilizing the relationships between relative density and SPT blow counts and between shear wave velocity and SPT blow counts.

Several relationships between relative density and SPT blow counts have been proposed in the past (Terzaghi and Peck 1967, Tokimatsu and Seed 1987, Idriss and Boulanger 2008). Data points collected by Mayne et al. (2002) and Tokimatsu and Seed (1987) are re-plotted in Fig. 3 showing the relationship between relative density and SPT blow counts corrected to an energy ratio of 60% with an overburden stress of 1 atm. $(N_1)_{60cs}$ is used as the abscissa in Fig. 3 to represent the equivalent clean sand $(N_1)_{60}$.

Expressions proposed by Terzaghi and Peck (1967) and Idriss and Boulanger (2008) as well as the curve by Tokimatsu and Seed (1987) are also plotted in Fig. 3. It can be seen that an average relationship can be better expressed by Eq. 11.

$$D_R = 100\sqrt{(N_1)_{60cs}/52} \quad (\%) \quad (11)$$

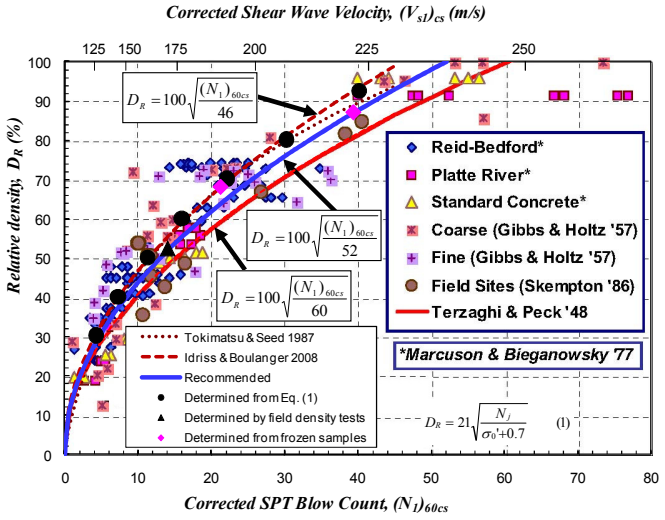

Fig. 3 Relationship between relative density, corrected SPT blow counts, and corrected shear wave velocity (data from Mayne et al. 2002 and Tokimatsu and Seed 1987)

Andrus et al. (2004) collected $(N_1)_{60cs}$ - $(V_{s1})_{cs}$ data pairs from different regions (Fig. 4). By nonlinear regression analysis, Andrus et al. (2004) obtained a power curve as shown by Eq. 12.

$$(V_{s1})_{cs} = 87.7[(N_1)_{60CS}]^{0.253} \quad (12)$$

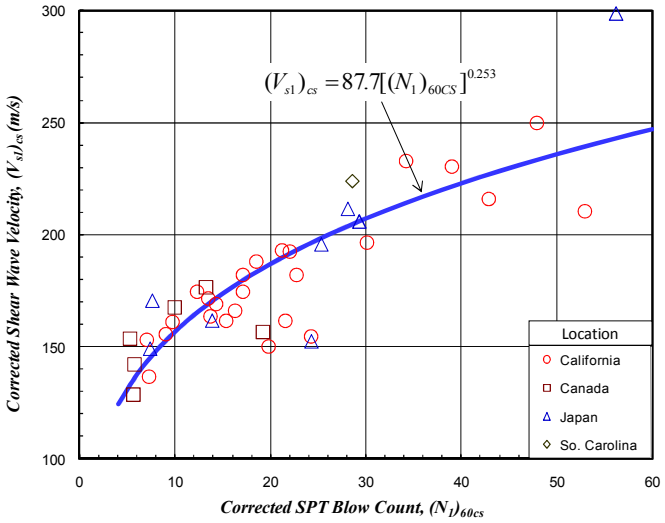

Fig. 4 Relationship between corrected shear wave velocity and corrected SPT blow counts for uncemented, Holocene sands (after Andrus et al. 2004)

By combining Eq. 11 and Eq. 12, the relationship between relative density and corrected shear velocity can be derived as shown in Eq. 13.

$$D_R = 17.974[(V_{S1})_{cs}/100]^{1.976} \quad (\%) \qquad (13)$$

The relationship between relative density and $(V_{s1})_{cs}$ shown in Eq. 13 is also plotted in Fig. 3.

Maximum shear strain. In the process of estimating the liquefaction-induced settlement, Ishihara and Yoshimine (1992) discovered that for a given value of relative density, the smaller the factor of safety, the larger the maximum shear strain. While at a given value of factor of safety less than unity, the larger the relative density, the smaller the maximum shear strain. A set of relationships was established as shown in Fig. 5.

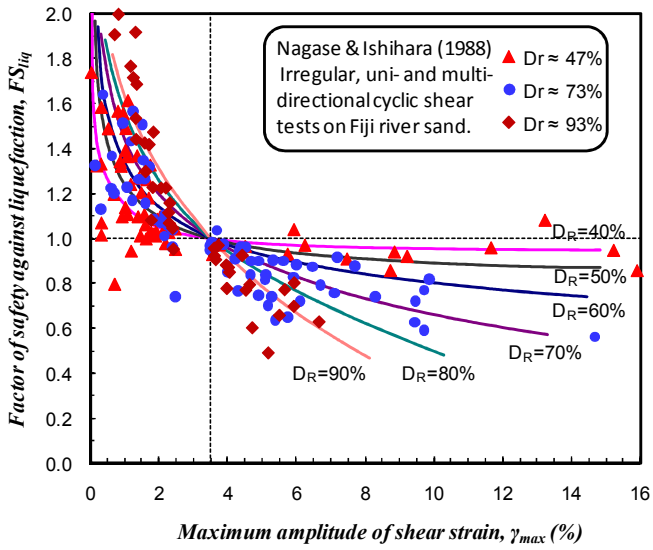

Fig. 5. Relationship between factor of safety and maximum amplitude of shear strain during irregular loading (after Ishihara and Yoshimine 1992, test data from Dr. Yoshimine)

Yoshimine et al (2006) approximated the curves in Fig. 5 with a hyperbolic function. This function was further combined with additional constrain of a limiting shear strain (Fig. 6) by Idriss and Boulanger (2008) to form the set of equations below for calculating the maximum shear strain.

$$\gamma_{max} = 0 \text{ , for } FS_{liq} \geq 2 \qquad (14a)$$

$$\gamma_{max} = \min\left(\gamma_{lim},\ 0.035(2 - FS_{liq})\left(\frac{1-F_\alpha}{FS_{liq}-F_\alpha}\right)\right)$$

$$\text{for } 2 > FS_{liq} \geq F_\alpha \qquad (14b)$$

$$\gamma_{max} = \gamma_{lim} \text{ , for } FS_{liq} < F_\alpha \text{ ,} \qquad (14c)$$

where γ_{max} is the maximum shear strain as a decimal, γ_{lim} is the limit of the maximum shear strain, and

$$F_\alpha = 0.032 + 4.7(D_R/100) - 6.0(D_R/100)^2 \qquad (15a)$$

The D_R should be limited to values ≥ 40% for use in Eq. 15a. By introducing Eq. 13, Eq. 15a becomes

$$F_\alpha = 0.032 + 0.836\left(\frac{(V_{s1})_{cs}}{100}\right)^{1.976} - 0.190\left(\frac{(V_{s1})_{cs}}{100}\right)^{3.952} \qquad (15b)$$

with $(V_{1s})_{cs}$ limited to values ≥ 150 (m/s).

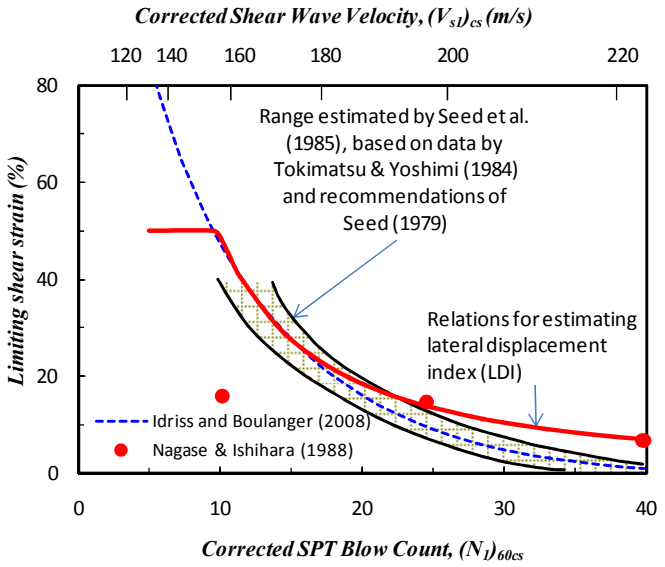

Fig. 6. Relationship between limiting shear strain, corrected SPT blow counts (modified after Idriss and Boulanger 2008), and corrected shear wave velocities

Idriss and Boulanger (2008) pointed out that the maximum shear strain that occurs at low factors of safety against liquefaction tend toward limiting values (for practical purposes) that decrease as the relative density of the sand increases. Fig. 6 shows the relationship between limiting shear strains and corrected SPT blow count, $(N_1)_{60cs}$. The original Idriss and Boulanger's relationship calculates a near 0 limiting shear strain at $(N_1)_{60cs}$ of 40 (approximately D_R of 93%). However, Nagase and Ishihara's (1988) test results indicate a maximum amplitude of shear strain of approximately 7% even at a relatively density of 93%. By combining Nagase and Ishihara's results, the limiting shear strain is modified as shown in Fig. 6. The corrected shear wave velocity, $(V_{s1})_{cs}$, is added to Idriss and Boulanger's (2008) original chart. With this modification, the relationship between limiting shear strain and corrected shear wave velocity can be expressed by the following equation.

$$\gamma_{lim} = \min\left[0.5,\ 7.05[(V_{s1})_{cs}/100]^{-5.53}\right] \geq 0 \qquad (16)$$

By combi
between t
replotted i
velocity. I
shear strai

in turn were underlain by interlayered clay, sand, and gravelly sand.

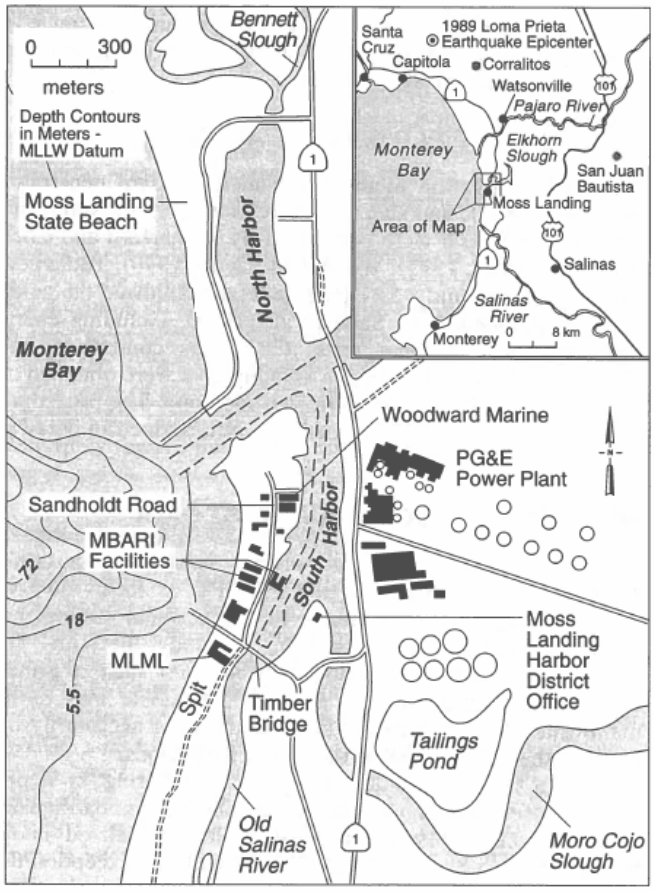

Fig. 9. Map of Moss Landing Area (after Boulanger et al. 1997)

The factor of safety against liquefaction, liquefaction-induced maximum shear strain, and LDI were calculated based on measured V_s data following the procedures described in the previous sections. The results are plotted in Fig. 10. For comparison, calculation results based on SPT and CPT data using the equations included in the MNO-12 "Soil Liquefaction during Earthquakes" (Idriss and Boulanger, 2008) are also illustrated in Fig. 10. The measured SPT blow counts and CPT tip resistance were converted to shear wave velocity for comparison. Results calculated by Idriss and Boulanger (2008) based on the same SPT data are also plotted in the graphs. It can be seen that the results calculated based on V_s data generally agree well with those calculated based on SPT and CPT data, especially with CPT data, and are consistent with the calculation results by Idriss and Boulanger (2008).

At the MBARI facility site, extensive ground deformations were observed along Sandholdt Road. Three slope inclinometers labeled SI-2, SI-4, and SI-5 were installed along the shoreline edge of Sandholdt Road, prior to the Loma Prieta earthquake. The readings of inclinometers before and after the earthquake indicate that the shoreline moved about 7.5 cm (SI-4) to 28 cm (SI-2) toward the harbor. V_s data as well as SPT and CPT data is available near SI-2. Based on the SPT log and laboratory test results, subsurface soils at this location generally consist of a poorly graded fine-grained sand layer with a fines content of between 2 and 3% to a depth of approximately 10.5 m below existing ground surface with 2 clayey silt interlayers with thickness of approximately 0.3 and 1 m, respectively. These in turn were underlain by soft to stiff clay with interlayered sand layers. The calculated results of the factor of safety, maximum shear strain, and LDI based on measured V_s data are plotted in Fig. 11. Similar to the first sample, results calculated based on SPT and CPT data are also illustrated in the graphs in Fig. 11. Other than the first sample, the results based on V_s data are closer to those based on SPT data.

To determine the coefficient C_h, calculated *LDI*'s were compared with lateral deformation observed from various locations in Moss Landing after the 1989 Loma Prieta earthquake. Fig. 12 shows the relationship. A C_h of 0.23 is obtained by regression analysis with an R-squared value of 0.74. With this correction, the calculated lateral spreading deformations are plotted in the right-most graph in Figs. 10 and 11 with comparison of observed data. As can be seen there is good agreement between observed data and calculated values.

It should be noted that C_h is affected by several factors. One of the factors could be the peak horizontal ground acceleration, a_{max}. As Idriss and Boulanger (2008) pointed out, the predicted deformations are sensitive at a certain range of a_{max}. Other factors affecting C_h and, further, the extent of lateral spreading are non-liquefied crust conditions (thickness and the cohesion) and surficial conditions (pavement etc.). The current methodology generally assumes a free movement of the non-liquefied crust without any resistance. These factors should be further evaluated in future studies.

CONCLUSIONS

A set of equations is proposed based on previous studies for calculating liquefaction-induced lateral spreading, extending to the application of shear wave velocity. The equations have been presented in the order of the calculation sequence. The proposed method was tested by utilizing data from two sites in Moss Landing where extensive surface deformations were observed after 1989 Loma Prieta earthquake. By using the proposed equations, the factor of safety against liquefaction, liquefaction-induced maximum shear strain, and *LDI* were calculated directly based on measured V_s data and compared with the results calculated based on SPT and CPT data using existing methods. The results indicate good agreement with the results obtained using the existing methods.

An important advantage of the proposed method is that with a small cost increase in the field investigation, it provides a verification of the predicted results using different field

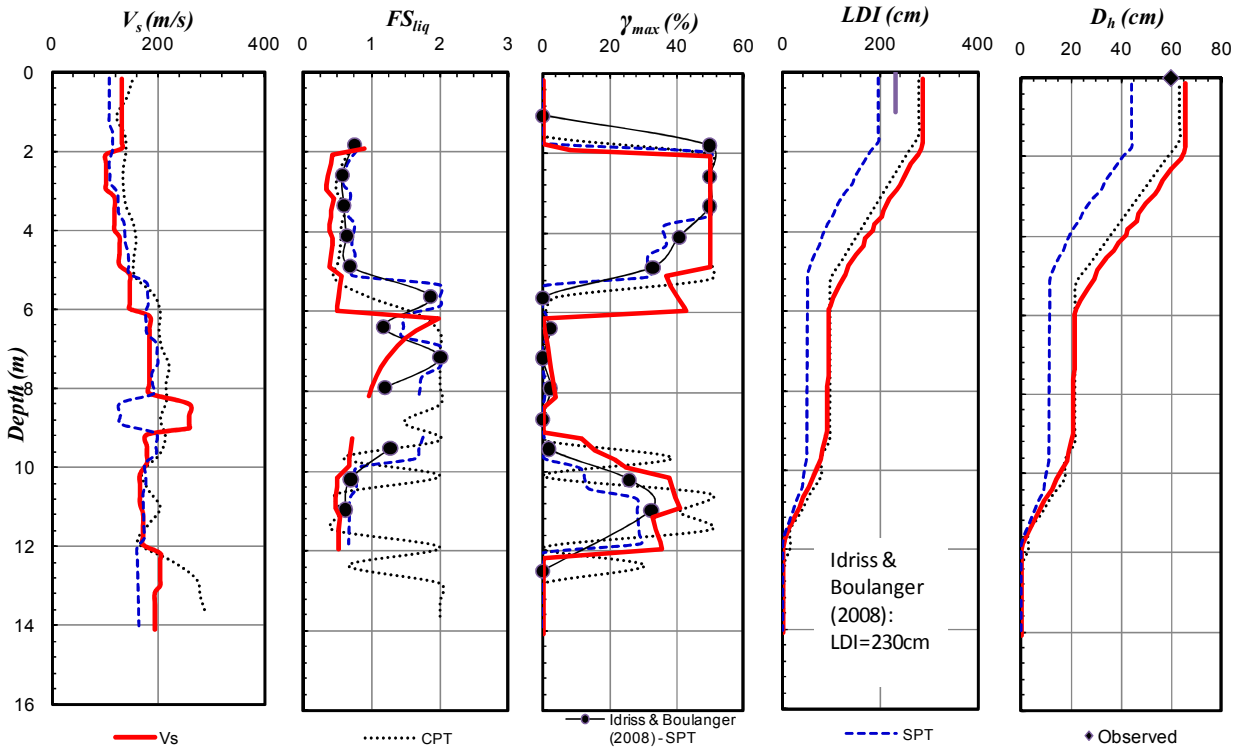

Fig. 10. Sample calculation of D_h at the Entrance Kiosk, Moss Landing State Beach, based on V_s data, comparing with CPT and SPT results as well as Idriss and Boulanger's (2008) calculation results based on SPT data (after Idriss and Boulanger 2008) and corrected shear wave velocity (a_{max}=0.25g)

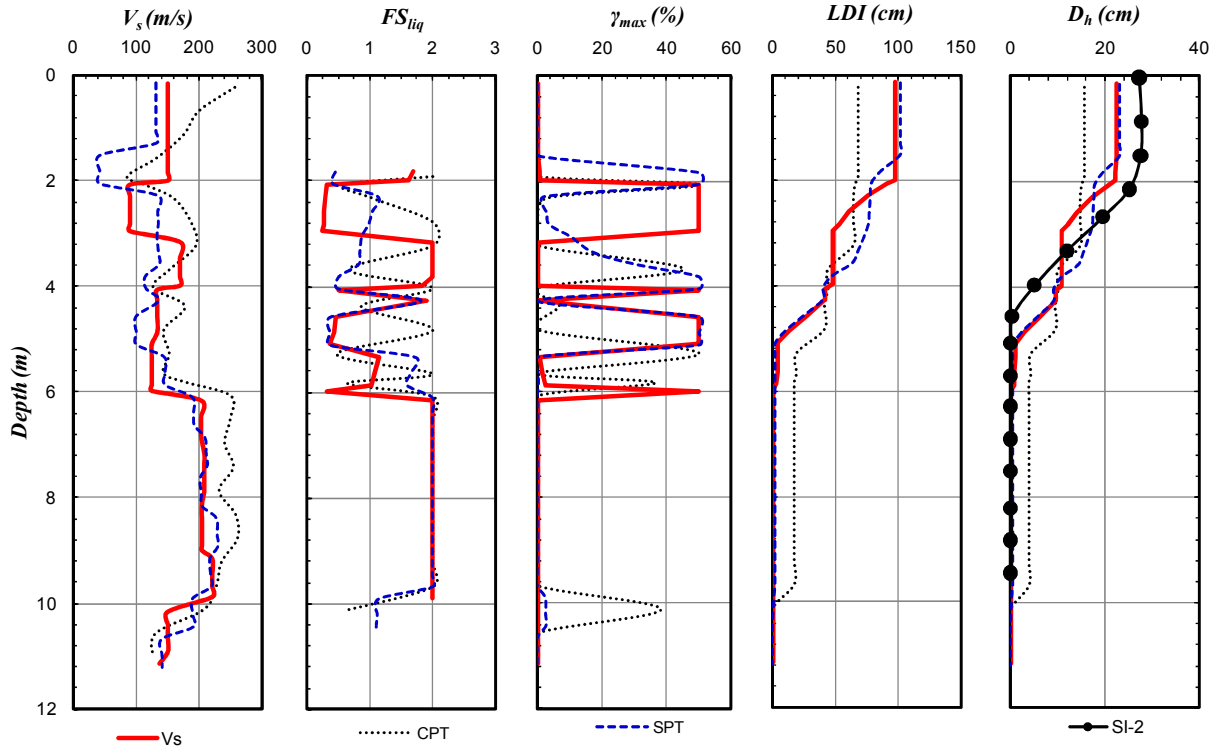

Fig.11. Sample calculation of D_h at Sandholdt Road, MBARI, based on V_s data, comparing with CPT and SPT results (a_{max}=0.25g)

investigation data. For example, other than just performing normal CPT sounding, both CPT and V_s data can be obtained during the same operation by using seismic cone. With an introduced coefficient C_h of 0.23, the calculated lateral spreading deformation agrees well with the observed data. However, it should be noted that this coefficient is affected by various factors. The sensitivity of the predicted liquefaction-induced spreading to various parameters should be evaluated as part of the analysis. Conditions of the non-liquefied crust (such as thickness, soil cohesion, and surface pavement), should also be considered in order to provide more reliable predicted values.

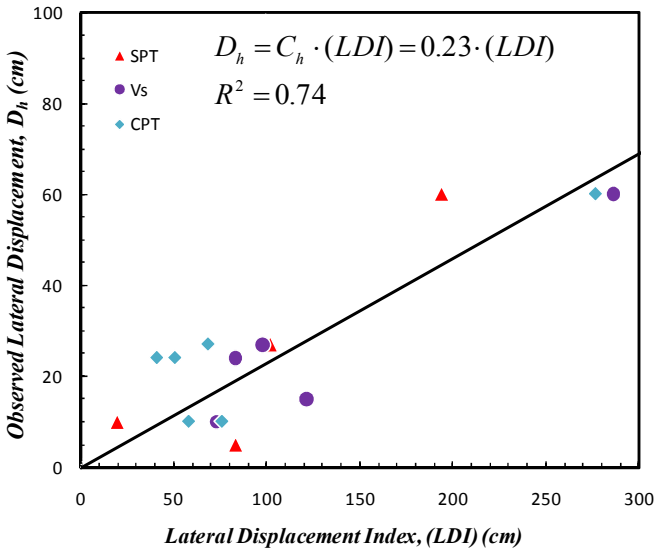

Fig. 12. Determination of coefficient C_h based on comparison of observed lateral spreading deformation and calculated LDI

ACKNOWLEDGMENTS

The author appreciates the support and help by Mr. Robert J. Johnson and Mr. Allen D. Evans in the preparation of this manuscript.

REFERENCES

Andrus, D.A. and K.H. Stokoe [2000]. "*Liquefaction Resistance of Soils from Shear Wave Velocity*", Journal of Geotechnical and Geoenvironmental Engineering, Vol. 126, No. 11, pp. 1015-1025

Andrus, D.A., P. Piratheepan, B.S. Ellis, J. Zhang, and C.H. Juang [2004]. "*Comparing Liquefaction Evaluation Methods Using Penetration-VS Relationships*", Soil Dynamics and Earthquake Engineering, Volume 24, Issues 9-10, October 2004, pp. 713-721

Arango, I. (1996). "*Magnitude Scaling Factors for Soil Liquefaction Evaluation*", J. Geotechnical Eng., ASCE 122(11), pp. 929-936

Bartlett, S.F. and T.L. Youd [1992]. "*Empirical analysis of horizontal ground displacement generated by liquefaction-induced lateral spread*": National Center for Earthquake Engineering Research Technical Report NCEER-92-0021, 114 pages.

Bartlett, S.F. and T.L. Youd [1995]. "*Empirical Prediction of Liquefaction-Induced Lateral Spread*": Journal of Geotechnical Engineering, ASCE, v. 121, No. 4, pp. 316-329.

Boulanger, R. W. and I. M. Idriss [2004]. "State normalization of penetration resistances and the effect of overburden stress on liquefaction resistance." *Proc., 11th Int. Conf. on Soil Dynamics and Earthquake Engineering, and 3rd Int. Conf. on Earthquake Geotechnical Engineering*, D. Doolin et al., eds., Stallion Press, Vol. 2, pp. 484-491.

Boulanger, R. W., I. M. Idriss, and L. H. Mejia [1995]. "Investigation and evaluation of liquefaction related ground displacements at Moss Landing during the 1989 Loma Prieta earthquake." Report No. UCD/CGM-95/02, Center for Geotechnical Modeling, Department of Civil and Environmental Engineering, University of California, Davis

Boulanger, R. W., L. H. Mejia, and I. M. Idriss [1997]. "*Liquefaction at Moss Landing during Loma Prieta Earthquake*", Journal of Geotechnical and Geoenvironmental Engineering, ASCE, 123(5): pp. 453-467.

Hamada, M., K. Wakamatsu, and S. Yasuda [1992]. "Liquefaction-induced ground deformation during the 1923 Kanto earthquake", *Case Studies of Liquefaction and Lifeline Performance during Past Earthquakes*, Vol. 1, *Technical Rep. NCEER-92-001*, National Center for Earthquake Engineering Research, Buffalo, N.Y.

Idriss, I.M. [1999]. "*An update to the Seed-Idriss simplified procedure for evaluating liquefaction potential*", in Proceedings, TRB Workshop on New Approaches to Liquefaction, Publication No.FHWA-RD-99-165,Federal Highway Administration, January.

Idriss, I. M., and R. W. Boulanger [2003a]. "Estimating K_α for use in evaluating cyclic resistance of sloping ground." *In Proc. 8th US-Japan Workshop on Earthquake Resistant Design of Lifeline Facilities and Countermeasures Against Liquefaction*, O'Rourke, Bardet, and Hamada, eds., Report MCEER-03-0003, pp. 449-468.

Idriss, I. M., and R. W. Boulanger [2003b]. "Relating K_α and K_σ to SPT blow count and to CPT tip resistance for use in evaluating liquefaction potential." *In Proceedings, 20th*

Annual Conference of Association of State Dam Safety Officials, ASDSO, Lexington, KY, September 8-10.

Idriss, I. M., and R. W. Boulanger, [2008]. "Soil Liquefaction During Earthquake", Earthquake Engineering Research Institute, EERI Publication MNO-12.

Ishihara, K., and M. Yoshimine [1992]. "*Evaluation of settlements in sand deposits following liquefaction during earthquakes*", Soils and Foundations 32(1), pp. 173–188.

Juang, C.H., T. Jiang, and R.D. Andrus [2002]. "*Assessing probability-based methods for liquefaction potential evaluation*", Journal of Geotechnical and Geoenvironmental Engineering, ASCE, 2002; 128(7), pp. 580-589.

Liao, S. C. and R. V. Whitman [1986], "*Overburden correction factors for SPT in sand*", J. Geot. Engrg., ASCE, 1986, 112(3), pp. 373-377.

Mayne, P.W., B. Christopher, R. Berg, and J. DeJong [2002]. "*Subsurface Investigations - Geotechnical Site Characterization*", Publication No. FHWA-NHI-01-031, National Highway Institute, Federal Highway Administration, Washington, D.C., 301 pages.

Nagase, H. and K. Ishihara [1988]. "*Liquefaction-induced compaction and settlement of sand during earthquakes*", Soils and Foundations, Vol. 28, No. 1, pp. 66-76.

NRC [1985]. "*Liquefaction of soils during earthquakes*", Report No. CETS-EE-001, National Academic Press, Washington, DC, USA

Rauch, A.F. [1997]. "*EPOLLS: An Empirical Method for Predicting Surface Displacements Due to Liquefaction-Induced Lateral Spreading in earthquakes*", Ph.D. dissertation, Virginia Polytechnic Institute and State University, VA.

Seed, H.B. [1983]. "*Earthquake Resistance Design of Earth Dams*", Symposium on Seismic Design of Earth Dams and caverns, ASCE, New York, pp. 41-64.

Seed, H.B., and I.M. Idriss [1971]. "*Simplified procedure fore valuating soil liquefaction potential*", J. Soil Mechanics and Foundations Div., ASCE 97 (SM9), pp. 1249–273.

Seed, H.B., and I.M. Idriss [1982]. "*Ground motions and soil liquefaction during earthquake*", Earthquake Engineering Research Institute, Oakland, CA, 134 pages.

Shamoto Y., J. Zhang and K. Tokimatsu [1998]. "*New charts for predicting large residual post-liquefaction ground deformation*", Soil Dynamics and Earthquake Engineering, Vol. 17, February 18, pp 427-438.

Terzaghi, K. and R. B. Peck [1967]. "*Soil Mechanics in Engineering Practice*", 2nd edn., John Wiley, New York, London, Sydney.

Tokimatsu, K. and Y. Yoshimi [1983]. "*Empirical correlations of soil liquefaction based on SPT N-values and fines content*", Soils and Foundations. 23(4), pp. 56-74.

Tokimatsu, K. and H.B. Seed [1987]. "*Evaluation of Settlements in Sands Due to Earthquake Shaking*", Journal of Geotechnical Engineering, Vol 113, No. 8, pp. 861-878.

Valsamis, A., G. Bouckovalas, and V. Dimitriadi, [2007]. "*Numerical evaluation of lateral spreading displacement in layered soils*", 4th International Conference on Earthquake Geotechnical Engineering. ISSMGE. Thessaloniki, Greece, June 25-28 Paper No. 1644

Varnes, D.J. [1978]. "Slope Movement Types and Processes", *Landslides – Analysis and Control*, Special Report 176, R. L. Schuster and R. J. Krizek (eds.), Trans. Research Board, Washington, D.C.

Wang, Z. [2008]. "*May 12, 2008 Sichuan, China Earthquake Reconnaissance*", University of Kentucky, Lexington, KY

Yi, F. [2009], "Case Study of CPT Application to Evaluate Seismic Settlement in Dry Sand", Manuscript submitted to *The 2nd International Symposium on Cone Penetration Testing*, Huntington Beach, California, USA, May 9-11, 2010.

Yoshimine, M., H. Nishizaki, K. Amano, and Y. Hosono [2006]. "*Flow Deformation of Liquefied Sand Under Constant Shear Load And Its Application To Analysis Of Flow Slide Of Infinite Slope*", Soil Dynamics and Earthquake Engineering, Vol.26, Issues 2-4, pp.253-264.

Youd, T.L., I.M. Idriss, R.D. Andrus, I. Arango, G. Castro, J.T. Christian, R. Dobry, W.D.L. Liam Finn, L.F. Harder, Jr. M.E. Hynes, K. Ishihara, J.P. Koester, S.S.C. Liao, W.F. Marcuson, III, G.R. Martin, J.K. Mitchell, Y. Moriwaki, M.S. Power, P.K. Robertson, R.B. Seed, K.H. Stokoe, II [1997]. "Summary Report", *Proceedings of the NCEER Workshop on Evaluation of Liquefaction Resistance of Soils*, National Center for Earthquake Engineering Research Technical Report NCEER-97-0022, pp. 1-40.

Zhang, G., P.K. Robertson, and R. W. I. Brachman [2004]. "*Estimating Liquefaction-Induced Lateral Displacements Using the Standard Penetration Test or Cone Penetration Test*", Journal of Geotechnical and Geoenvironmental Engineering, ASCE, August, 2004, 861-871